Supporting Information

Ag@g-C_3N_4/MoS_2 Heterostructure for Efficient Photocatalytic Oxygen Evolution Under Visible Light Irradiation

Tayyab Sohail Aslam,[a,b] Jinsong Chen,[a,b] Umm Y Umna,[a,b] Kamran Muzaffar,[a,b] Ateeq Ur Rehman,[a,b] Syeda Andleeb Zahra Naqvi,[a,b] Rahul Anil Borse,[a,b,c*] Yangyang Feng,[a,b,c*] and Yaobing Wang[a,b,c*]

[a] CAS Key Laboratory of Design and Assembly of Functional Nanostructures, and Fujian Provincial Key Laboratory of Nanomaterials, State Key Laboratory of Structural Chemistry, Fujian Institute of Research on the Structure of Matter, Chinese Academy of Sciences, Fuzhou 350002, Fujian, P. R. China.

[b] University of Chinese Academy of Sciences, Beijing 100049, P. R. China.

[c] Fujian Science and Technology Innovation Laboratory for Optoelectronic Information of China, Fuzhou 350108, Fujian, P. R. China.

Email: rahulchem90@gmail.com; fengyangyang@fjirsm.ac.cn; wangyb@fjirsm.ac.cn

1. Materials and Methods:

1.1. Materials

Bis(acetylacetonato)dioxomolybdenum(VI) ($MoO_2(acac)_2$), sulfur powder (100% mesh), oleylamine (OM, 70%) were purchased from Aladdin. trioctylphosphine (TOP, 90%), toluene (99.8%), Graphitic carbon nitrides (g-C_3N_4, 95%), silver nitrate ($AgNO_3$, >99), acetone and methanol (AR) were purchased from Shanghai Macklin Biochemical Technology Company limited, China and used as received without further purification.

1.2. Methods:

1.2.1. Synthesis of Ag@g-C_3N_4/MoS_2

Ag-OM solution: 0.5 mmol/1 mmol/2 mmol of $AgNO_3$ was added to 10 mL of OM with magnetic stirrer and heated at 80°C for 1 h to prepare 0.5 mmol/1 mmol/2 mmol Ag-OM solution. Afterward, the solution was purged with N_2 for 15 minutes, and then sealed the vial for further used in reaction.

Mo-OM solution: 1 mmol of $MoO_2(acac)_2$ was added to 10 mL of OM and then degassed before heating at 120 °C for 30 min and then increased the temperature to 200 °C with magnetic stirrer at 500 rpm. This solution was then used for the reaction.

Ag@g-C_3N_4/MoS_2 was synthesized using a two-step method. In the first step, Ag@MoS_2 was synthesized by a wet chemical method. In this step, 48 mg of sulfur powder was added to 26 of mL OM in a double neck flask. The mixture was degassed and then heated with a magnetic stirrer. Heating started from room temp to 120 °C and maintained for 1 h, then increased temp to 230 °C to inject Ag-OM quickly. The temperature decreased to 200 °C for 1 h/2 h and 1 mL of Mo-OM solution was injected. Reaction was considered as completed and cooled down to the room temperature. In the end, mixture was centrifuged with ethanol and three times with toluene at 8000 rpm for 5 min. Finally, sample was dried in vacuum oven at 60° for 2 h to get the Ag@MoS_2.

The same method was used in the second step to synthesize the Ag@g-C_3N_4/MoS_2. 3:1 of Ag@MoS_2 and of g-C_3N_4 mixed with 10 mL of OM in double neck flask. The mixture was degassed and then heated at 120 °C with magnetic stirrer for 1 h under N_2 condition. After 1 h, the temperature was increased to 200 °C, and 1 mL of TOP was injected. Reaction cooled down to the room temperature. The mixture was centrifuged with toluene three times at 8000 rpm for 5 min each time. The sample was collected and dried it in vacuum oven at 60 °C for 2 h to get the Ag@g-C_3N_4/MoS_2 photocatalyst.

1.2.2. Synthesis of Ag@g-C_3N_4

Ag@g-C_3N_4 was synthesized by using calcination method. Typically, $AgNO_3$ and g-C_3N_4 mixture (1:15 ratio) was transferred to a covered crucible and heated in tube furnace from 25 °C to 300 °C at a rate 5 °C/min followed by 300 °C to 550 °C at a rate of 1 °C/min for 4 h. After the natural cooling down, the resultant Ag@g-C_3N_4 was collected for characterizations and test the performance.

1.2.3. Synthesis of g-C_3N_4/MoS_2

MoS_2@g-C_3N_4 was synthesized by using calcination method with ratio 3:1 of MoS2 and g-C_3N_4 at 550°C in tube furnace. Followed the same process to set the temp of tube furnace as used for the synthesis of Ag@g-C_3N_4. In the end, grind the sample for characterizations and test the performance.

2. Characterizations:

Rigaku Miniflex 600 used to record XRD with diffraction intensity data for 2θ from 15 ~75° and 5 ~ 85° with scanning speed of 5 deg per min with 2θ step increment of 0.01°.

Escalab 250Xi instrument used to record X-ray photoelectron spectroscopy (XPS) from Thermo Scientific equipped with an Al Kα micro-focused X-ray source.

Scanning Electron Microscope (FE-SEM, HITACHI UHR SU8200) was used to scan Ag@g-C_3N_4/MoS_2 with 10 kV acceleration voltage.

Transmission Electron Microscopy (TEM, 7650B, Hitachi) with 200kV accelerating voltage was used to get HR-TEM images.

UV–vis diffuse reflectance spectroscopy (UV–vis DRS) of Ag@g-C_3N_4/MoS_2, Ag@g-C_3N_4, g-C_3N_4 and MoS_2 were tested on Shimadzu UV-2450 spectrophotometer.

Fourier transform infrared spectroscopy (FTIR) spectra of Ag@g-C_3N_4/MoS_2 and Ag@g-C_3N_4 were tested on Thermo Nicolet IS5 FT-IR (ATR) spectrometer. Conditions were ambition with ranging from 500 cm^{-1} to 4000 cm^{-1}.

All photocatalytic tests were performed on Labsolar-6A. Circulation system was gas-closed with temp 5°C. 300W Xe lamp (PLSSXE300) was used for irradiation (λ > 420 nm). Gas chromatograph (GC Techcomp, GC7900) was used to determine O_2 production.

Thermal stability test of Ag@g-C_3N_4/MoS_2 was performed on thermal analyzer HS-TGA-101 (HESON, China) under N_2 conditions with a heating rate of 10 °C min^{-1} from 25 °C to 800 °C .

3. Apparent Quantum Yield (AQY) calculation:

The wavelength-dependent POER of Ag@g-C_3N_4/MoS_2 was performed to measure the apparent quantum yields (AQY) according to the following formula. The highest AQY was observed for the Ag@g-C_3N_4/MoS_2 at 400 nm and decreased with longer wavelengths, in accordance with the UV-DRS, indicating that the absorption of photons is crucial in the OER processes.

For example: λ = 400 nm

$$N = \frac{E\lambda}{hc} = \frac{9 \times 26.4 \times 10^{-3} \times 3600 \times 400 \times 10^{-9}}{6.626 \times 10^{-34} \times 3 \times 10^{8}}$$

$$N = 1.72 \times 10^{21}$$

$$AQY = \frac{4 \times the\ number\ of\ evolved\ O_2\ molecule}{N} \times 100$$

$$AQY = \frac{4 \times 0.096244 \times 6.02 \times 10^{23}}{1.72 \times 10^{21}} \times 100 = 1.34\%$$

3. Photoelectrochemical Characterization:

Electrochemical station (CHI 660E) was used to measure Mott Schottky, EIS and transient photocurrent response.

3.1. Sample preparation for steady-state PL absorption spectra:

6 mg of Ag@g-C_3N_4/MoS_2, Ag@g-C_3N_4 and MoS_2 were dispersed in 6 mL of ethanol absolute.

3.2. Testing and sample preparation for Mott Schottky, EIS, and transient photocurrent response:

10 mg of Ag@g-C_3N_4/MoS_2, Ag@g-C_3N_4, MoS_2, and g-C_3N_4 was dispersed separately in 0.8 mL of ethanol absolute 0.2 mL of Nafion. Three electrode electrochemical cells were employed for testing with Ti electrode (working electrode), Ag/AgCl (reference electrode), and Pt (counter electrode). 0.5 M Na_2SO_4 (electrolyte solution). Visible light ($\lambda > 420$ nm) was used for transient photocurrent response.

4. Photocatalytic oxygen evolution reaction (POER):

5 mg of sample (Ag@g-C_3N_4/MoS_2, g-C_3N_4/MoS_2 and Ag@g-C_3N_4) and $AgNO_3$ was dispersed in 100 mL of water separately. A series of samples was prepared by dispersing 5 mg of Ag@g-C_3N_4/MoS_2 with different amounts of $AgNO_3$ and different sacrificial agents in 100 mL of water.

5. **Powder X-ray diffraction (PXRD):**

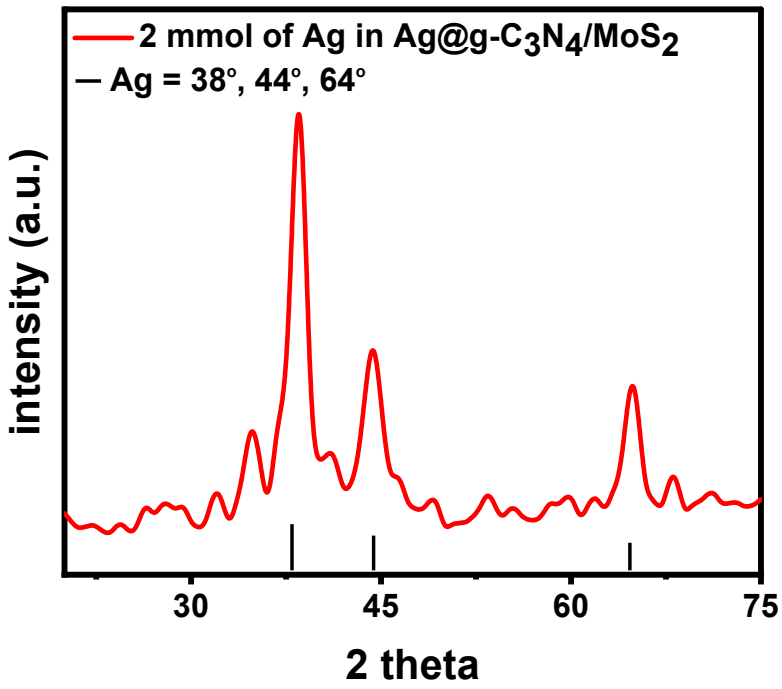

Figure S1: PXRD of Ag@g-C_3N_4/MoS_2 with 2 mmol concentration of Ag.

As shown in figure S1, high crystalline Ag was synthesized as compare to 1 mmol concentration of Ag in Ag@g-C_3N_4/MoS_2 under the similar synthesis conditions.

6. Powder X-ray diffraction (PXRD):

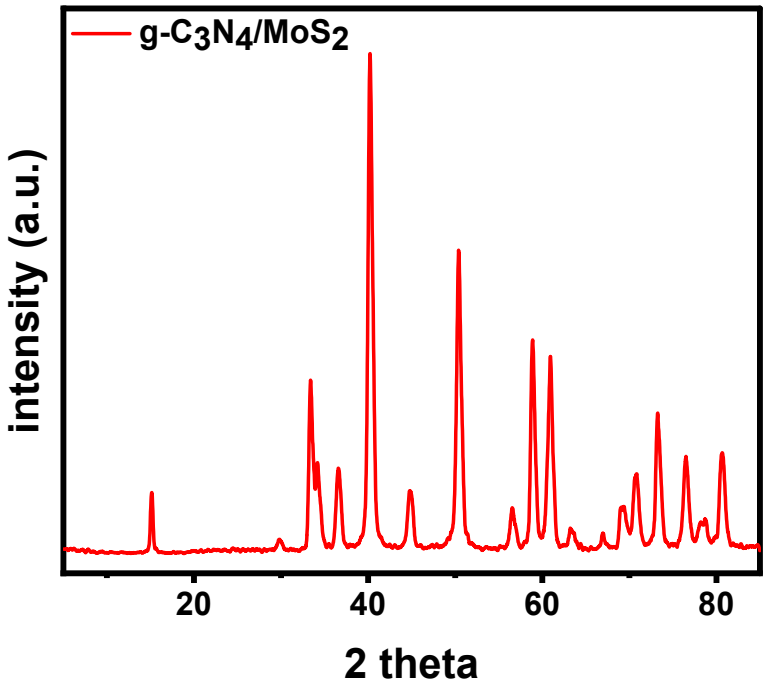

Figure S2: XRD of g-C_3N_4/MoS_2.

7. Transmission Electron Microscopy (TEM) images after 2 h growth of Ag particles:

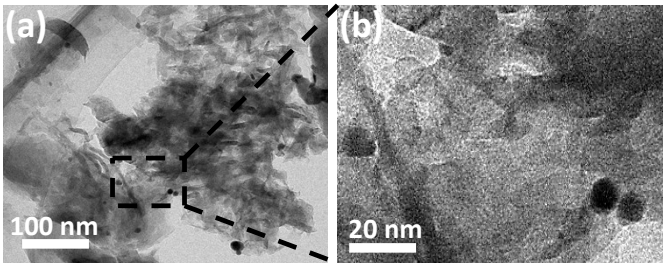

Figure S3: TEM images of Ag@g-C_3N_4/MoS_2 after 2 h growth of Ag particles (a) 100 nm scale (b) 20 nm scale.

8. Transmission Electron Microscopy (TEM) images after 1 h growth of Ag particles:

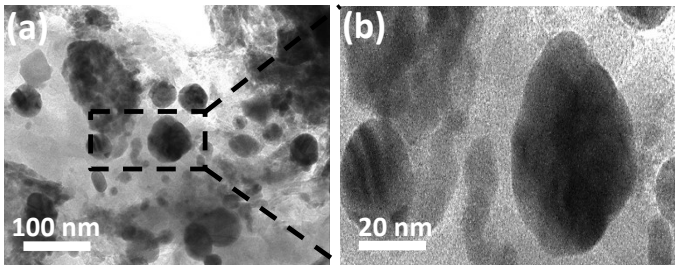

Figure S4: TEM images of Ag@g-C_3N_4/MoS_2 after 1 h growth of Ag particles (a) 100 nm scale (b) 20 nm scale.

In figure S3 and S4, Ag particles have different size due to reaction time after injecting the Ag-OM to reaction system (OM solution).

9. X-ray Photoelectron Spectroscopy:

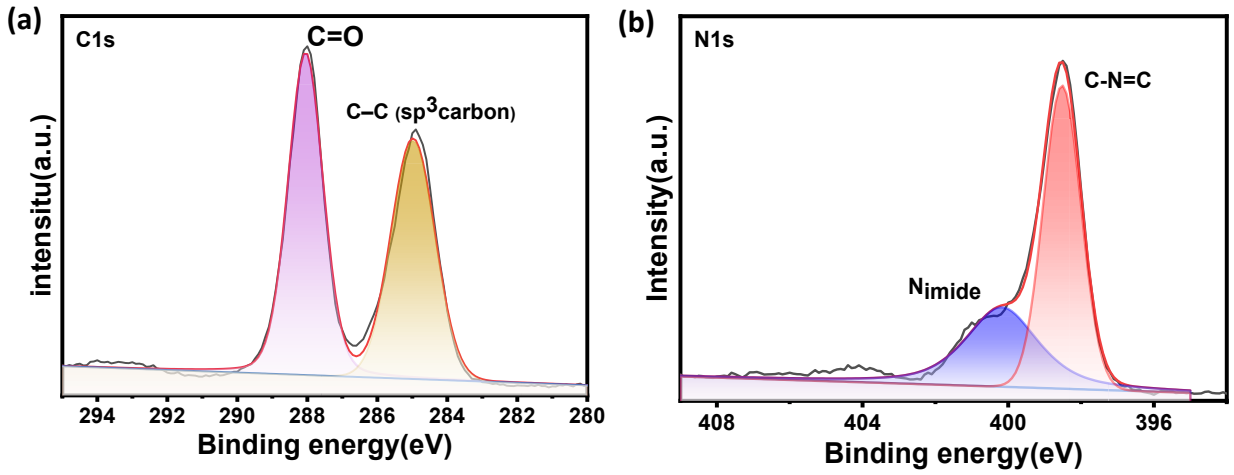

Figure S5: XPS of (a) C1s and (b) N1s.

10. Tauc Plot, energy band gap structure diagram, and Mott-Schottky plot of Ag@g-C_3N_4/MoS_2 and Ag@g-C_3N_4:

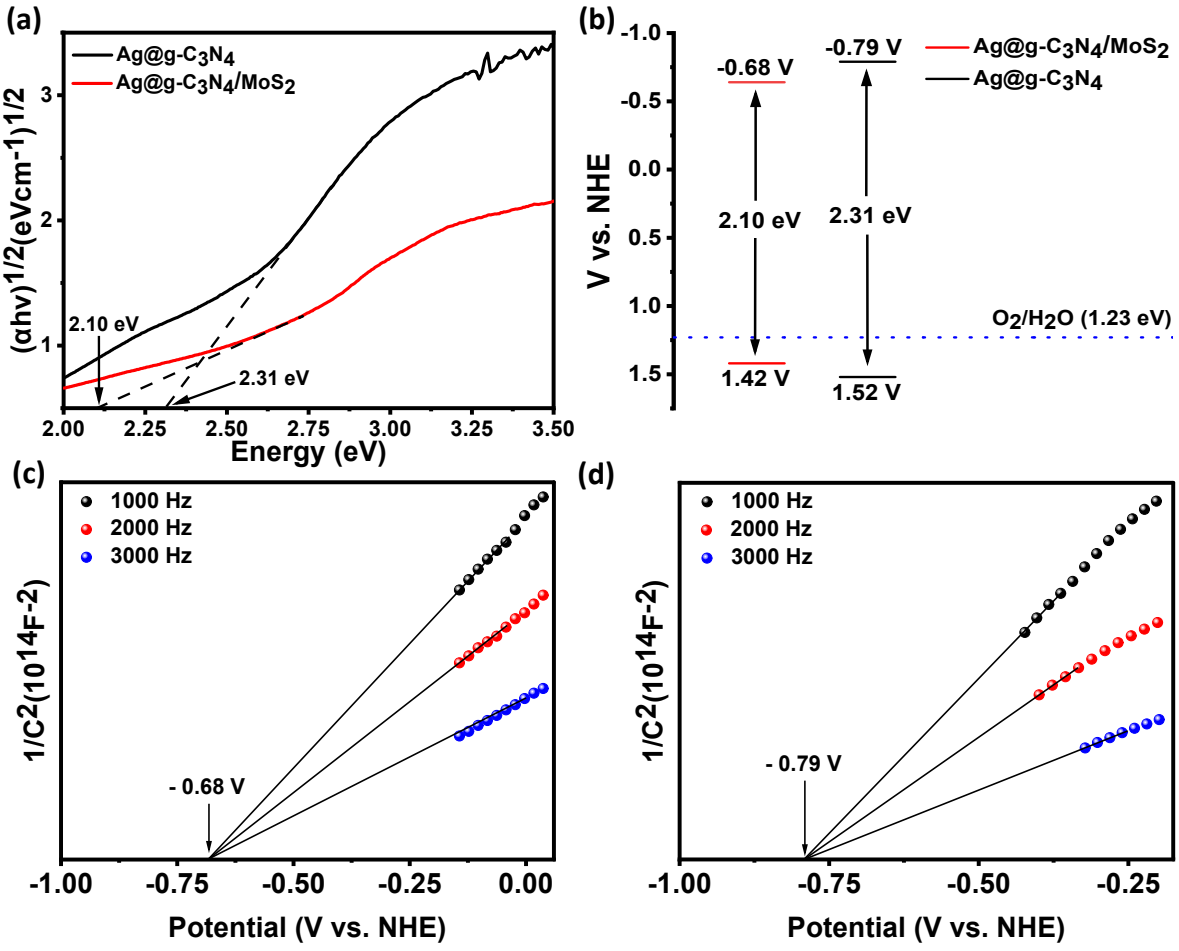

Figure S6: Ag@g-C_3N_4/MoS_2 and Ag@g-C_3N_4 (a) Tauc Plot. (b) energy band gap structure diagram. Mott-Schottky plot of (c) Ag@g-C_3N_4/MoS_2 and (d) Ag@g-C_3N_4.

11. Mott-Schottky plots:

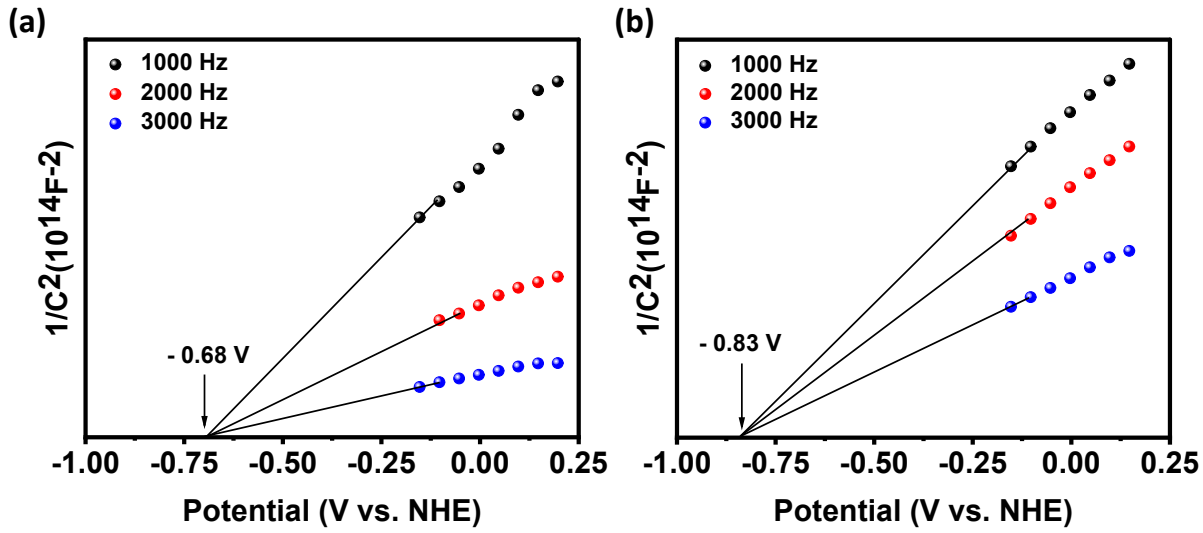

Figure S7: Mott-Schottky plots of (a) g-C_3N_4 and (b) MoS_2.

Mott-Schottky of g-C_3N_4 and MoS_2 tested under three different frequencies (figure S7).

12. POER with different concentration of Ag:

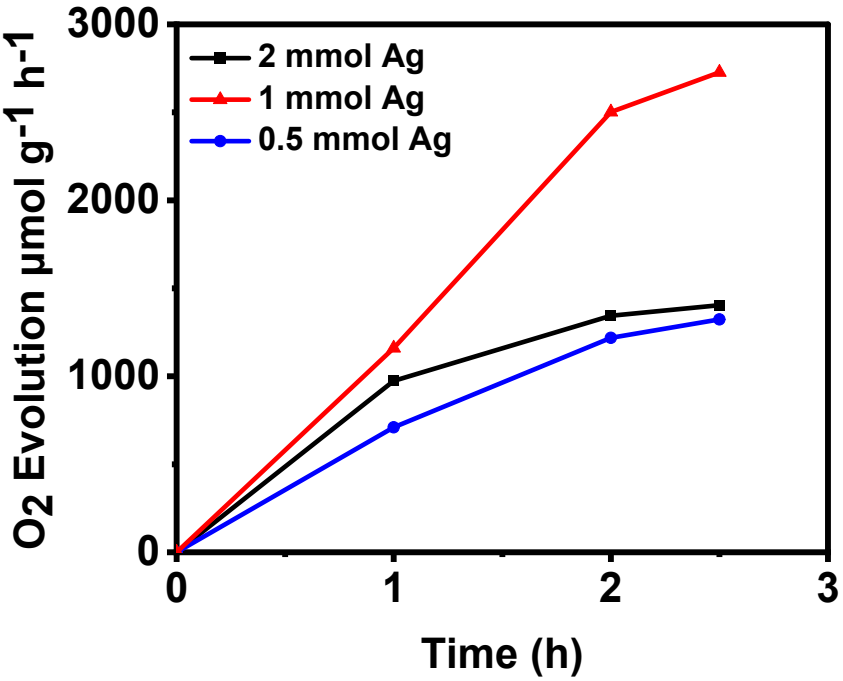

Figure S8: POER under different Ag concentrations in the synthesis of Ag@g-C_3N_4/MoS_2.

The resulting data of figure S8 of the lowest photoactivity revealed that increased Ag concentration blocked the active sites and formed electron clusters in Ag@g-C_3N_4/MoS_2. Relatively, rough distribution on the surface due to high Ag concentration made difficult for light harvesting to lead to photocatalytic activity. While decreasing the Ag concentration is also not effective because active sites are not enough and demonstrated poor conductivity for efficient photocatalytic activity.

13. Ag particles size dependent photocatalytic activity:

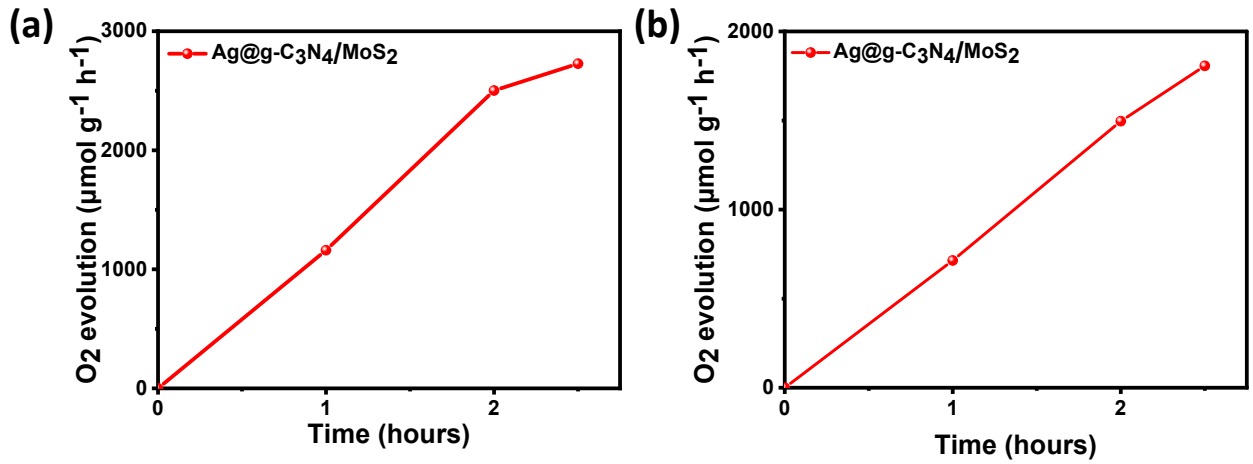

Figure S9: Photocatalytic performance with (a) 22.13 nm size of Ag particles and (b) 50.68 nm size of Ag particles.

14. Cyclic and Stability tests for O_2 of Ag@g-C_3N_4/MoS_2:

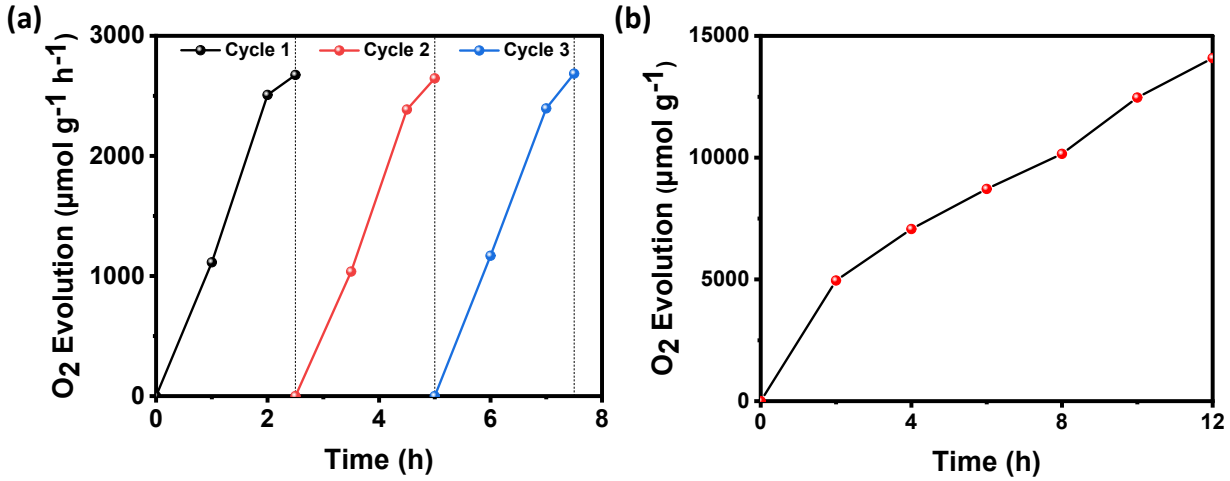

Figure S10: O_2 evolution tests of Ag@g-C_3N_4/MoS_2 (a) cyclic test and (b) stability test.

15. Thermal stability test using thermal gravimetric analysis (TGA):

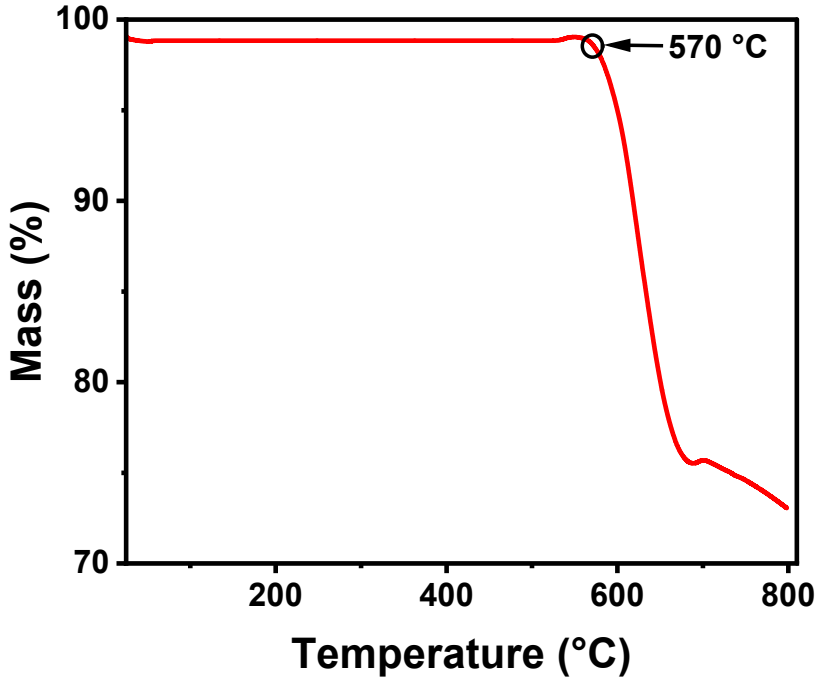

Figure S11: TGA curve of Ag@g-C_3N_4/MoS_2.

Mass loss started at 570 °C, and only 27% of the mass was lost at a temperature of 800 °C (figure S11).

16. POER with different amounts of sacrificial agent ($AgNO_3$):

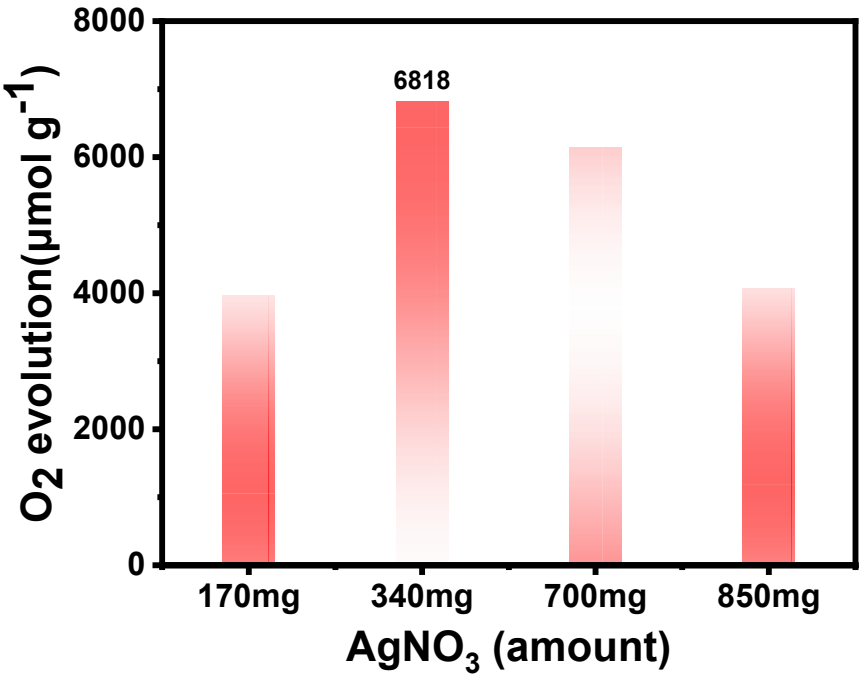

Figure S12: POER rate of Ag@g-C_3N_4/MoS_2 with different amounts of $AgNO_3$.

17. POER with different sacrificial agents:

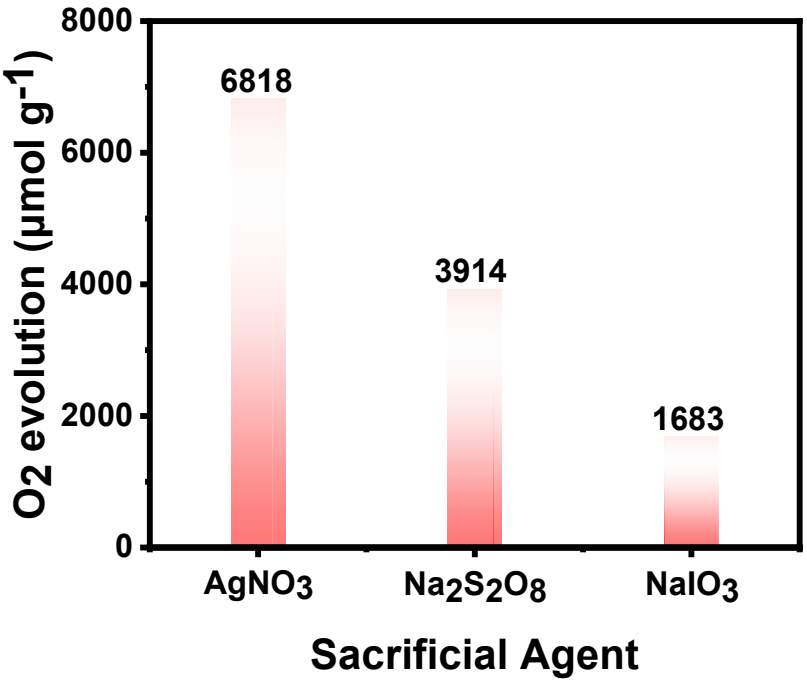

Figure S13: POER rate of Ag@g-C_3N_4/MoS_2 with different sacrificial agents.

18. PL spectra:

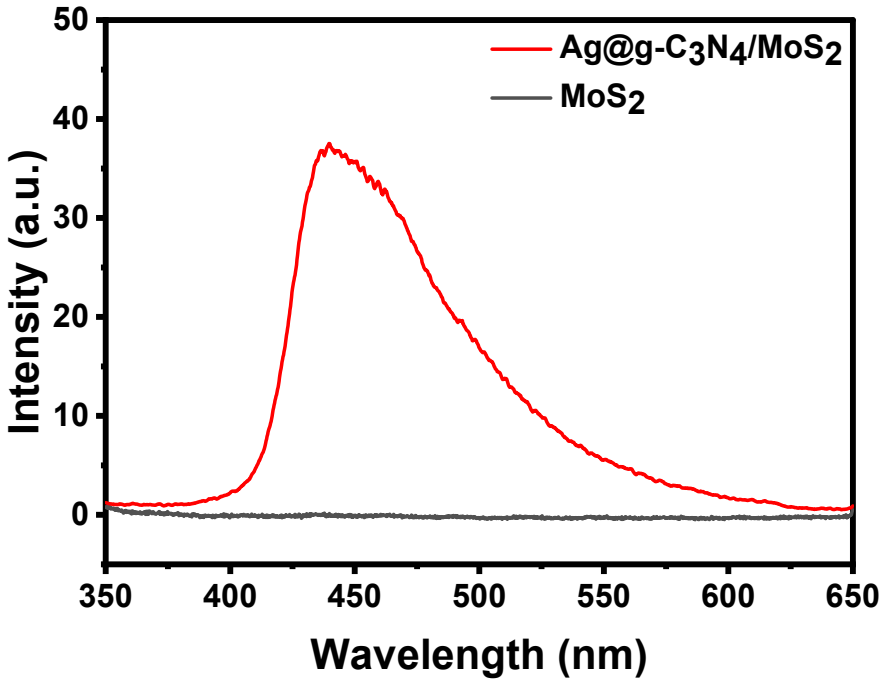

Figure S14: PL spectra of MoS_2 and Ag@g-C_3N_4/MoS_2 to demonstrate Z-scheme experimentally.

Figure S14 revealed PL spectra to investigate Ag@g-C_3N_4/MoS_2 heterostructure and the formation of Z-scheme, as it is confirmed by the appearance peak at 430 nm.

19. EIS plot:

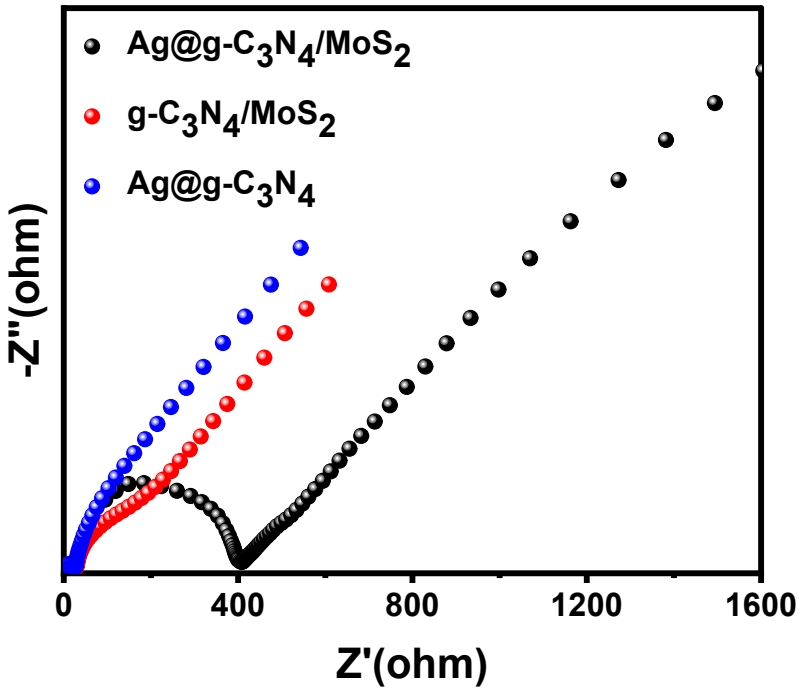

Figure S15: EIS plots of Ag@g-C_3N_4/MoS_2, g-C_3N_4/MoS_2 and Ag@g-C_3N_4.

20. Supporting Table:

Table S1. Photocatalytic oxygen production comparison of g-C_3N_4, MoS_2 and Ag based catalysts.

Catalyst	Co-catalyst / sacrificial agent	O_2 evolution rate	Reference
Ag@g-C_3N_4/MoS_2	2mMol $AgNO_3$	2727 µmol g^{-1} h^{-1}	This Work
g-C_3N_4/MoS_2	2mMol $AgNO_3$	1292 µmol g^{-1} h^{-1}	This Work
Ag@g-C_3N_4	2mMol $AgNO_3$	849 µmol g^{-1} h^{-1}	This Work
g-C_3N_4	Pt	20 µmol	[1]
boron-doped and nitrogen-deficient g-C_3N_4	0.01M $AgNO_3$, 3% wt of Co $(OH)_2$	561.2 µmol g^{-1} h^{-1}	[2]
Co/g-C_3N_4	0.01M $AgNO_3$,	13.0 µmol h^{-1}	[3]
$Co(OH)_2$/gC_3N_4	0.01M $AgNO_3$, 3% wt of Co $(OH)_2$	27.4 µmol h^{-1}	[4]
Ag_3PO_4/ g-C_3N_4	$AgNO_3$	29 µmol L^{-1} g^{-1} h^{-1}	[5]
MFG ($(MoS_2$, γ-$Fe_2O_3)$/graphene)	0.01 M $AgNO_3$	4400 µmol g^{-1} h^{-1}	[6]
Ag_3PO_4/MoS_2	$AgNO_3$ aqueous solution (100mL, 10 g/L)	201.6 µmol L^{-1} g^{-1} h^{-1}	[7]
g-C_3N_4/MoS_2/Ag_3PO_4	$AgNO_3$ (1 g)	35 µmol L^{-1}	[8]
MoS_2/Ag dots/Ag_3PO_4	0.01 M $AgNO_3$	1542 µmol g_{cat}^{-1}	[9]

21. References:

1. X. Wang, S. Blechert and M. Antonietti, *ACS Catal.*, 2012, **2**, 1596-1606.
2. D. Zhao, C. L. Dong, B. Wang, C. Chen, Y. C. Huang, Z. Diao, S. Li, L. Guo and S. Shen, *Adv. Mater.*, 2019, **31**, 1903545.
3. G. Zhang, C. Huang and X. Wang, *Small*, 2015, **11**, 1215-1221.
4. T. Xiong, W. Cen, Y. Zhang and F. Dong, *ACS Catalysis*, 2016, **6**, 2462-2472.
5. X. Yang, L. Tian, X. Zhao, H. Tang, Q. Liu and G. Li, *Appl. Catal. B: Environ.*, 2019, **244**, 240-249.
6. A. Li, Y. Liu, X. Xu, Y. Zhang, Z. Si, X. Wu, R. Ran and D. Weng, *RSC Adv.*, 2020, **10**, 17154-17162.
7. X. Cui, X. Yang, X. Xian, L. Tian, H. Tang and Q. Liu, *fChem.*, 2018, **6**, 373723.
8. L. Tian, X. Yang, X. Cui, Q. Liu and H. Tang, *Appl. Surf. Sci.*, 2019, **463**, 9-17.
9. Z. Wang, X. Xu, Z. Si, L. Liu, Y. Liu, Y. He, R. Ran and D. Weng, *Appl. Surf. Sci.*, 2018, **450**, 441-450.